Single Hydration of the Peptide Bond: The Case of the Vince Lactam

6 AUTHORS, INCLUDING:

Patricia Écija
Universidad del País Vasco / Euskal Herriko U…
31 PUBLICATIONS 195 CITATIONS

SEE PROFILE

Francisco J. Basterretxea
Universidad del País Vasco / Euskal Herriko U…
33 PUBLICATIONS 185 CITATIONS

SEE PROFILE

Alberto Lesarri
Universidad de Valladolid
170 PUBLICATIONS 2,368 CITATIONS

SEE PROFILE

Emilio José Cocinero
Universidad del País Vasco / Euskal Herriko U…
111 PUBLICATIONS 1,174 CITATIONS

SEE PROFILE

Single Hydration of the Peptide Bond: The Case of the Vince Lactam

Patricia Écija,[†] Francisco J. Basterretxea,*,[†] Alberto Lesarri,[‡] Judith Millán,[§] Fernando Castaño,[†] and Emilio J. Cocinero*,[†]

[†]Departamento de Química Física, Facultad de Ciencia y Tecnología, Universidad del País Vasco (UPV/EHU), Campus de Leioa, Ap. 644, E-48080 Bilbao, Spain

[‡]Departamento de Química Física y Química Inorgánica, Facultad de Ciencias, Universidad de Valladolid, E-47011 Valladolid, Spain

[§]Departamento de Química, Facultad de Ciencias, Estudios Agroalimentarios e Informática, Universidad de La Rioja, E-26006 Logroño, Spain

ⓢ Supporting Information

ABSTRACT: 2-Azabicyclo[2.2.1]hept-5-en-3-one (ABH or Vince lactam) and its monohydrated complex (ABH···H_2O) have been observed in a supersonic jet by Fourier transform microwave spectroscopy. ABH is broadly used in the synthesis of therapeutic drugs, whereas the ABH···H_2O system offers a simple model to explain the conformational preferences of water linked to a constrained peptidic bond. A single predominant form of the Vince lactam and its singly hydrated complex have been detected, determining the rotational constants, centrifugal distortion constants, and nuclear quadrupole coupling tensor. The monohydrated complex is stabilized by two hydrogen bonds (C=O···H−O and N−H···O) closing a six-membered ring. The complexation energy has been estimated to be ~10 kJ mol^{-1} from experimental results. In addition, the observed structure in the gas phase has been compared with solid-phase diffraction data. The structural parameters and binding energies of ABH···H_2O have also been compared with similar molecules containing peptide bonds. Ab initio (MP2) and density functional (M06-2X and B3LYP) methods have supported the experimental work, describing the rotational parameters and conformational landscape of the title compound and its singly hydrated complex.
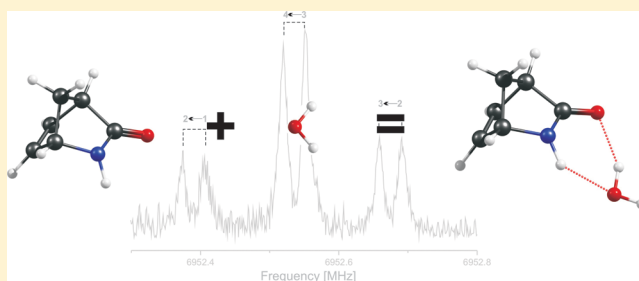
INTRODUCTION

The subtle intramolecular factors controlling the structure of small building blocks such as hydrogen bonds or orbital interactions can be determined by spectroscopic means and can help to understand the more complicated three-dimensional architecture of biomolecular ensembles.[1] These experiments thus help in discerning between intrinsic molecular properties and those imposed by the medium and also allow the addition of surrounding molecules in a controlled fashion. As a consequence, we can construct a progressive picture of the intermolecular interactions acting between the bare molecule and the solvated structures. In this respect, amides and lactams (cyclic amides) provide a model to describe the peptidic bond or the structural core of antibiotics such as penicillins and cephalosporins, which are built upon the β-lactam moiety. The study of hydrogen bonding in these systems is crucial to understand water binding to biological structures in solution, such as proteins,[2] DNA base pairs,[3] or carbohydrates.[4,5]

As most biologically relevant molecules have very low pressures at ambient temperature and are also thermally labile, methods have been devised to carry intact molecules into the gas phase. In particular, supersonic expansions cool molecules to very low temperatures (T_{rot} < 5 K), thus depopulating the majority of rovibrational quantum states and simplifying the molecular spectra. Supersonic expansions can also generate a substantial population of weakly bound intermolecular complexes, which can be characterized without interactions with other species. These techniques are usually combined with spectroscopic methods, such as optical and electronic spectroscopies or mass spectrometry. Microwave (MW) spectroscopy, a traditionally powerful method for determining precise gas-phase structures of small molecules, has benefited from supersonic jet Fourier-transform methods and complementary sample preparation techniques such as laser ablation or electric discharge sources. These advances have allowed rapid extension of the variety and size of amenable molecular systems by MW spectroscopy, allowing discrimination among conformers,[6] tautomers, or even isotopomers[7] of moderate-size molecules. Gas-phase rotational spectroscopy takes advantage of the extremely large accuracy of frequency measurements, which provide the most detailed vision of the molecular structure through accurately determined moments of inertia. The obtained molecular parameters serve also as a test for quantum mechanics calculations, especially the new emerging density functional methods. To date, we have used rotational spectroscopy to study the conformational and structural

properties of different families of compounds of chemical and biological interest, such as tropanes,[8] norbornanes,[9] vanillins,[10−12] and sugars.[13]

This work presents the study of 2-azabicyclo[2.2.1]hept-5-en-3-one (ABH), also known as Vince lactam. The molecule is a norbornane-based structure in which a carbon atom in position 2 of norbornane has been replaced by an amino group, a carbonyl functional group appears on the adjacent C-3 atom, and a double bond has been added between carbon atoms in positions 5 and 6 in the six-membered ring (see Scheme 1).

Scheme 1. Molecular Formula and Atom Labeling of the Vince Lactam
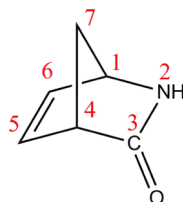
ABH belongs to the family of bicyclic γ-lactams and is widely used in organic and medicinal chemistry as a precursor molecule or chemical intermediate. The structural and unsaturated features of this molecule have been exploited in the preparation of compounds such as carbocyclic nucleosides and other non-nucleoside therapeutic drugs with medicinal applications in the treatment of diabetes, hepatitis, HIV, or cancer.[14−16] ABH is a chiral molecule and can exist in two enantiomers that are spectroscopically undistinguishable. Lactams deserve interest also because they exhibit π-conjugation between the amino and carbonyl moieties of the amide group[17] that has been shown to arise from inductive and resonance effects and which can vary for different geometries between the two groups. It is thus interesting to consider how hydration of the peptidic group is affected by the rigid ring in ABH. To date, there are only a few structural studies on hydrated species of simple amides and lactams, such as formamide···$(H_2O)_{1,2}$,[18] N-methylformamide···H_2O,[19] 2-azetidinone···$(H_2O)_{1,2}$,[20] uracil···H_2O,[21] thymine···H_2O,[22] or 2-pyridone···H_2O.[23] Some information about the nature of various intramolecular interactions in the bicyclic structure of ABH was described through its HeI photoelectron spectrum.[24] It was established that there is no transannular interaction between the π-moiety and the amide group. The crystal structure of (−)-2-azabicyclo[2.2.1]hept-5-en-3-one has been reported.[25] The X-ray diffraction study shows that the molecules are linked by hydrogen bonds between N−H and C=O groups, forming ribbons, although this structure is affected by neighboring ABH molecules. Previous quantum mechanics calculations on ABH[24] were performed at the B3LYP/6-31G* level.

EXPERIMENTAL AND COMPUTATIONAL DETAILS

The experiments were carried out in the 4−18 GHz region using the Fourier-transform microwave (FT-MW) spectrometer built at the Universidad del País Vasco (UPV/EHU),[10] which is based on the Balle−Flygare design.[26] Commercial samples of solid (±)-azabicyclo[2.2.1]hept-5-en-3-one (98%) were used without further purification. A solid sample of ABH was placed inside a custom metal reservoir at the injection nozzle and was transferred to the gas phase by slightly heating

(45 °C) the reservoir with a resistive wire. The vaporized ABH was transferred to the spectrometer chamber by flowing pure Ne (99.997%) through the reservoir at stagnation pressures of ∼3 bar. The mixture expanded through a 0.8 mm diameter nozzle in a high-vacuum chamber evacuated by a rotary and a diffusion pump, reaching 1×10^{-7} mbar in standby conditions.

To record the spectrum of the monohydrated complex, a reservoir containing a sample of liquid water at ambient temperature soaked up in glass wool was attached to the Ne carrier flow tube to take up water vapor that was flowed through the ABH reservoir. In this case the reservoir was heated to 55 °C to increase the signal/noise ratio.

The gas mixture enters the vacuum chamber via pulses of ∼250 μs duration, forming a supersonic expansion. A sequence of 1 μs low-power (<150 mW) microwave pulses excite the molecules inside a Fabry−Perot MW resonator. The molecular spontaneous emission is detected in the time domain and is subsequently Fourier-transformed to obtain the frequency spectra. All transitions appear split due to the Doppler effect arising from the coaxial arrangement of the jet and resonator axis. The frequency measurement accuracy is better than 3 kHz, and transitions can be fully resolved for lines as close as 10 kHz.

For both the ABH monomer and ABH···H_2O complex, we performed ab initio (MP2) and density functional theory (DFT) molecular orbital calculations as an aid to spectral line searching and assignment, as well as to calculate the most relevant features of the potential energy surfaces of both systems. The obtained experimental rotational constants allowed us to test the predictive performance of MP2 and DFT methods. The well-known B3LYP and the recently released M06-2X density functional methods[27−29] have been employed. The B3LYP functional is one of the most successful in terms of overall performance, whereas M06-2X is a highly parametrized metahybrid functional empirically accounting for dispersive interactions at reasonable computational cost. Standard Pople's triple-ζ 6-311++G(d,p) basis functions were employed in all the methods, as implemented in the Gaussian 09 software package.[30] For calculations involving water complexes, we took into account the basis set superposition error using the counterpoise correction[27] via the following relationship:

$$E_d = E_{AB}^{\alpha \cup \beta}(AB) - E_A^{\alpha}(A) - E_B^{\beta}(B)$$
$$- (E_A^{\alpha \cup \beta}(AB) + E_B^{\alpha \cup \beta}(AB) - E_A^{\alpha}(AB) - E_B^{\beta}(AB)) \quad (1)$$

where A, B, and AB stand for both monomers and the complex, respectively, α, β, and $\alpha \cup \beta$ are the basis sets for A, B, and AB, respectively, and the subscript stands for the optimized geometry (e.g., $E_A^{\alpha \cup \beta}(AB)$ represents the energy of the complex calculated at the optimized geometry of monomer A in the $\alpha \cup \beta$ basis set).

RESULTS

Rotational Spectrum of ABH. As a starting point to look for spectral lines, quantum chemical calculations guided the experiment. We used a strategy based on our previous experience, using both MP2 and DFT computations to predict the most intense rotational transitions. The calculations showed that ABH gives rise to a single conformational structure, as expected from the steric constraints present in the bicyclo motif. Once a few intense rotational transitions were detected and assigned, a preliminary set of rotational constants was
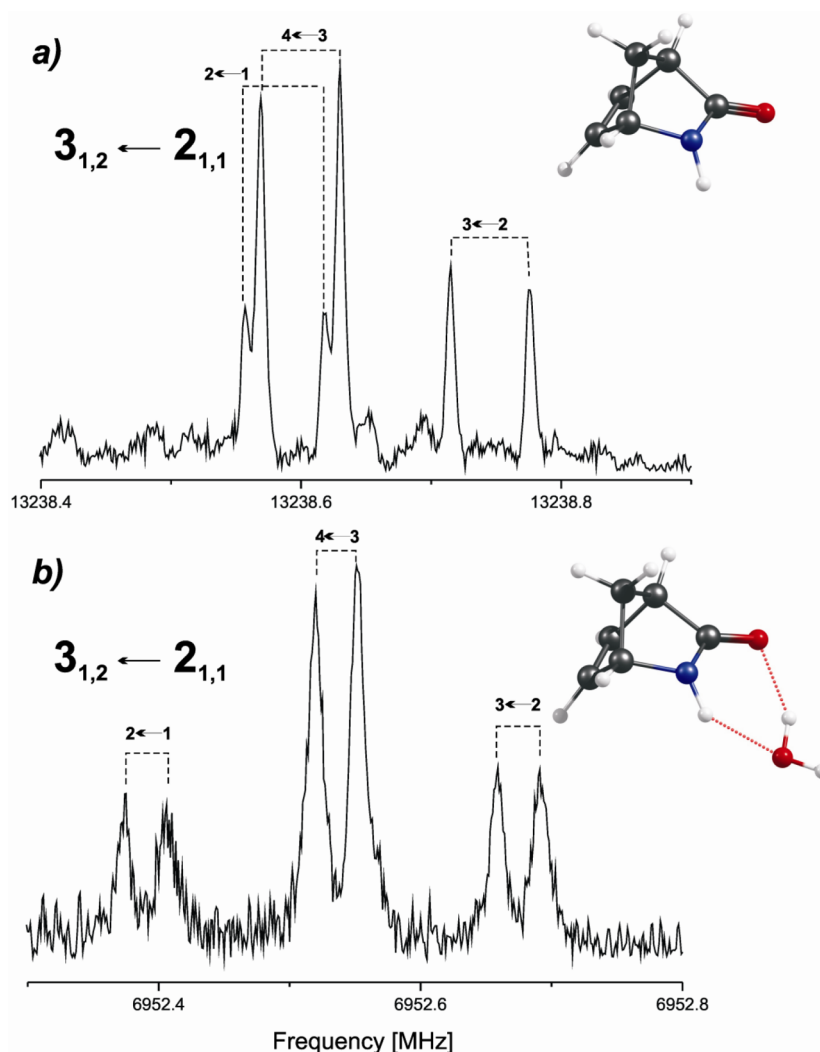
Figure 1. The $3_{1,2} \leftarrow 2_{1,1}$ ($J'_{K'_{-1},K'_{+1}} \leftarrow J''_{K''_{-1},K''_{+1}}$) rotational transition in (a) ABH and (b) the ABH···H_2O complex. The hyperfine components $F' \leftarrow F''$ are also shown. Note that each line is doubled (with a spacing of ca. 60 kHz in a)) as a result of the Doppler effect in the supersonic expansion. The computed structures are also shown.

obtained, allowing the prediction and detection of additional (weaker) transitions. The whole set of recorded transitions was used to obtain more accurate rotational constants. All lines in the spectrum could be assigned to a single species.

All rotational transitions belonging to ABH exhibit small hyperfine splittings with components separated by less than 1−2 MHz, as shown in Figure 1. A total number of 73 components belonging to 24 rotational transitions were measured. All observed transitions are R-type ($\Delta J = +1$), with nine lines obeying μ_a-type selection rules ($^aR_{0,1}$, where the subscripts refer to ΔK_{-1} and ΔK_{+1} quantum number changes, respectively), nine lines obeying μ_b-type selection rules ($^bR_{-1,1}$, $^bR_{1,1}$, and $^bR_{1,-1}$), and the remaining six lines obeying μ_c-type selection rules ($^cR_{1,0}$ and $^cR_{-1,2}$). The lower state rotational quantum numbers of the observed transitions were in the $0 \leq J \leq 3$, $0 \leq K_{-1} \leq 2$, and $0 \leq K_{+1} \leq 3$ ranges. All measured lines and their assignments are given in Table S1 of the Supporting Information.

The splittings observed in the R-type transitions arise from ^{14}N nuclear quadrupole coupling interactions, giving $F' \leftarrow F''$ hyperfine transitions, where F ($= J + I, J + I − 1, ..., |J − I|$) represents the rotational (J) and nuclear spin ($I(^{14}N) = 1$) total

angular momentum. Mostly $\Delta F = +1$ transitions were observed, together with a few $\Delta F = 0$ transitions.[31]

The fitting of the rotational parameters, including the diagonal elements (χ_{aa}, χ_{bb}, χ_{cc})[31] of the nuclear quadrupole coupling tensor, used a Watson semirigid rotor Hamiltonian in the S reduction.[32] The nuclear quadrupole coupling tensor elements $\chi_{\alpha\beta}$ are expressed in the principal inertial axes ($\alpha, \beta = a, b, c$) and are linearly related to the molecular electric field gradients at the quadrupolar nucleus.[31]

Table 1 shows the determined parameters, which include rotational (A, B, C) and centrifugal distortion constants, together with the nuclear quadrupole coupling tensor elements $\chi_{\alpha\alpha}$ ($\alpha = a, b, c$). The MP2- and DFT (B3LYP and M06-2X)-predicted values are shown in the same table. The three methods foresee a single minimum in the potential energy landscape of the molecule, as could be envisaged from its rigid structure. The degree of agreement between experimental and predicted rotational parameters is very good. Thus, an univocal correspondence between the experimentally determined species and the calculated structure was straightforward for all the methods used. The MP2- and DFT-calculated structures are shown in Tables S2−S4 of the Supporting Information. The

Table 1. Rotational Parameters of ABH and Comparison with the Quantum-Mechanical Predictions Using MP2 and Density Functional (M06-2X and B3LYP) Models

	experiment	theory, MP2 [M06-2X] B3LYP
A^a/MHz	3792.33565(21)^d	3795.0 [3811.8] 3799.4
B/MHz	2258.31637(23)	2259.8 [2270.2] 2244.6
C/MHz	2058.91648(20)	2056.9 [2070.0] 2047.1
D_J/kHz	0.2190(94)	0.19 [0.19] 0.18
D_K/kHz	[0.0]^e	0.29 [0.30] 0.30
D_{JK}/kHz	[0.0]	0.13 [0.12] 0.13
d_1/Hz	[0.0]	−7.34 [−7.57] −7.53
d_2/Hz	[0.0]	0.83 [1.00] 0.93
$\|\mu_a\|$/D		3.73 [3.92] 3.95
$\|\mu_b\|$/D		0.71 [0.82] 0.87
$\|\mu_c\|$/D		0.25 [0.17] 0.20
$\|\mu_{TOT}\|$/D		3.81 [4.01] 4.05
χ_{aa}^b/MHz	2.0029(12)	2.03 [2.11] 2.15
χ_{bb}/MHz	−0.7089(37)	−0.85 [−0.82] −0.72
χ_{cc}/MHz	−1.2940(37)	−1.17 [−1.29] −1.43
χ_{ab}/MHz	[0.0]	0.76 [0.84] 0.85
χ_{ac}/MHz	[0.0]	−1.11 [-1.22] −1.26
χ_{bc}/MHz	[0.0]	3.02 [3.20] 3.28
N^c	73	
σ/kHz	2.56	

^{a}Rotational constants (A, B, C), Watson's quartic centrifugal distortion constants in the S reduction (D_J, D_K, D_{JK}, d_1, d_2), and electric dipole moment components (μ_α, $\alpha = a$, b, c; 1 D $\approx$ 3.336 × 10^{-30} C m) referred to the principal inertial axes. ^{b}Nuclear quadrupole coupling tensor in the principal inertial axes ($\chi_{\alpha\beta}$, α, $\beta = a$, b, c). ^{c}Number of transitions (N) and rms deviation (σ) of the fit. ^{d}Standard error in parentheses in units of the last digit. ^{e}Value set to zero in the fit.

standard deviation of the global fit (2.6 kHz) is below the assumed uncertainty of the frequency measurements.

Rotational Spectrum of ABH···H$_2$O. The addition of gaseous water to the Ne carrier gas flowing through the ABH reservoir resulted in the appearance of additional weaker lines in the microwave spectra, about 1 order of magnitude weaker than the most intense rotational transitions of bare ABH. MP2 and DFT (B3LYP and M06-2X) calculations were carried out for the ABH···H$_2$O complex to aid in the conformational search, similarly to ABH. In this way a total number of 52 components of 20 rotational transitions could be assigned due to the ABH···H$_2$O complex. An example of the $3_{1,2} \leftarrow 2_{1,1}$ transition is shown in Figure 1. Only one single conformer of ABH···H$_2$O was observed. All measured lines and their assignments are given in Table S5 of the Supporting Information.

The lines measured comprise lower state quantum numbers in the $1 \leq J \leq 5$, $0 \leq K_{-1} \leq 3$, and $0 \leq K_{+1} \leq 4$ ranges. All transitions are R-type, most of them (16) μ_a-type, with a few (4) μ_b-type. As for ABH, hyperfine splittings due to ^{14}N are observed in the spectral lines. Only $\Delta F = +1$ transitions were detected for the complex species. The fitting of the rotational parameters and nuclear quadrupole coupling tensor diagonal elements proceeded analogously to that for ABH. The obtained experimental results appear in Table 2. The standard deviation of the global fit (1.9 kHz) is again below the assumed uncertainty of the frequency measurements.

The computed structures of ABH···H$_2$O present a variety of possible conformations which differ in the relative location of the H$_2$O moiety with respect to the bare ABH. The computed

Table 2. Rotational Parameters of ABH···H$_2$O

	experiment
A^a/MHz	2907.58230(86)^d
B/MHz	1184.84658(24)
C/MHz	1082.52148(28)
D_J/kHz	0.3617(28)
D_K/kHz	2.114(78)
D_{JK}/kHz	−0.394(12)
d_1/Hz	23.1(34)
d_2/Hz	[0.0]^e
χ_{aa}^b/MHz	2.0935(43)
χ_{bb}/MHz	1.799(11)
χ_{cc}/MHz	−3.892(11)
N^c	54
σ/kHz	1.94

^{a}Rotational constants (A, B, C) and Watson's quartic centrifugal distortion constants in the S reduction (D_J, D_K, D_{JK}, d_1, d_2). ^{b}Nuclear quadrupole coupling tensor in the principal inertial axes ($\chi_{\alpha\beta}$, α, $\beta = a$, b, c). ^{c}Number of transitions (N) and rms deviation (σ) of the fit. ^{d}Standard error in parentheses in units of the last digit. ^{e}Value set to zero in the fit.
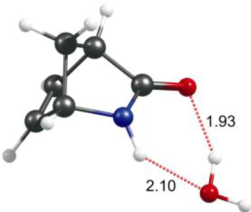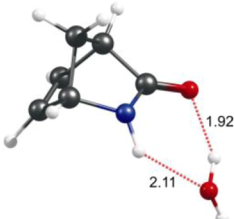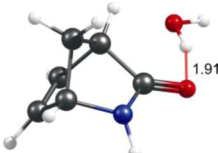
spectroscopic parameters of the lowest energy conformers of ABH···H$_2$O are presented in Table 3.

The global minimum in all methods reproduced the same structure (conformer 1). This complex is stabilized by two hydrogen bonds in which the water molecule bonds to the carbonyl through a C=O···H−O bond and the cycle is closed by a N−H···O link, creating a stable six-membered ring, as shown in Table 3 (see also Tables S6−S8 in the Supporting Information for atomic coordinates). The calculations predict an additional potential energy minimum (conformer 2) almost isoenergetic with the global minimum with a very low energy barrier (estimated at 1.0 kJ mol^{-1} for MP2 calculations; see Figure S1 in the Supporting Information). This structure differs only in the orientation of the water hydrogen atom not participating in hydrogen bonds and will presumably relax collisionally to the global minimum. Alternatively, interconversion between both structures will take place as the low barrier will be easily surmounted due to the zero-point energies of both conformers. The next energy minimum was predicted for all three methods at about 5 kJ mol^{-1} above the global minimum and corresponds to a structure (conformer 3 in Table 3) in which the water molecule bonds to ABH via a C=O···H−O hydrogen bond and a weak C−H···O bond to the aliphatic ring, but without contacts of the water oxygen to the amino group. Due to this more flexible geometry, the rotational constants calculated for conformer 3 show larger differences for the three theoretical methods than the previous conformations. Conformer 3 was discarded when comparing the predicted rotational constants and the nuclear quadrupole coupling tensor elements with the experimental values (differences are around 5% in A and B and up to 90% in χ_{bb}). The rest of the predicted conformers lie at relative energies higher than 17 kJ mol^{-1}, precluding their observation in the jet experimental conditions.

In view of the previous data, it is reasonable to assign the species observed in the supersonic expansion to conformer 1. A comparison of the computed rotational constants and quadrupole tensor elements in Table 3 with the experimental values in Table 2 gives an overall good agreement. The possibility of observing conformer 2, lying slightly above the global

Table 3. Computed Rotational Constants, Electric Dipole Moments, Nuclear Quadrupole Coupling Tensor Components, and Zero-Point-Energy-Corrected Relative Energies for the Lower Energy Conformers of ABH···H$_2$O^a

	Conformer 1	*Conformer 2*	*Conformer 3*
	MP2 / M06-2X / B3LYP	MP2 / M06-2X / B3LYP	MP2 / M06-2X / B3LYP
A / MHz	2850.3 / 2915.6 / 2911.2	2889.1 / 2930.5 / 2936.2	2777.9 / 2671.2 / 2879.6
B / MHz	1209.3 / 1205.5 / 1180.2	1193.6 / 1201.0 / 1172.2	1253.2 / 1390.4 / 1162.8
C / MHz	1102.3 / 1099.5 / 1078.9	1087.9 / 1095.1 / 1071.2	1067.6 / 1146.1 / 1019.6
$|\mu_a|$ / D	2.00 / 2.19 / 2.38	2.61 / 2.52 / 2.79	3.11 / 2.68 / 3.83
$|\mu_b|$ / D	1.21 / 1.32 / 1.35	1.31 / 1.45 / 1.43	0.03 / 0.61 / 0.36
$|\mu_c|$ / D	0.75 / 0.86 / 0.96	1.04 / 0.83 / 0.86	0.52 / 0.81 / 0.084
$|\mu_{TOT}|$ / D	2.46 / 2.70 / 2.89	3.10 / 3.03 / 3.25	3.15 / 2.87 /3.85
χ_{aa} / MHz	2.13 / 2.21 / 2.30	2.12 / 2.19 / 2.28	1.69 / 1.27 / 2.14
χ_{bb} / MHz	1.74 / 1.92 / 2.07	1.81 / 1.94 / 2.02	0.16 / -0.21 / 0.72
χ_{cc} / MHz	-3.87 / -4.13 / -4.19	-3.93 / -4.13 / -4.30	-1.85 / -1.06 / -2.86
χ_{ab} / MHz	-0.31 / -0.32 / -0.29	-0.31 / -0.32 /-0.29	-0.90 / -1.55 / -0.33
χ_{ac} / MHz	-0.18 / -0.40 / -0.39	-0.42 / -0.52 / -0.58	-0.95 / -1.53 / -0.26
χ_{bc} / MHz	0.69 /0.48 / 0.54	0.33 / 0.31 / 0.26	-2.91 / -2.96 / -3.01
ΔE / kJ mol^{-1}	0.0 / 0.0 / 0.0	0.5 / 0.1 / 0.0	5.7 / 6.2 / 5.9
ΔG^{353} / kJ mol^{-1}	0.0 / 0.0 / 0.0	0.7 / 0.2 / 0.0	0.1 / 5.2 / 1.6

^{a}The distances (Å) between hydrogen-bonded atoms are also shown.

minimum, was examined. The structural differences between conformer 1 and conformer 2 involve only a displacement of a single H atom not participating in the hydrogen bonds, so the change in the rotational constants is very small and interconversion between both conformations is expected to take place easily. The comparison with the experimental rotational constants slightly (but quite confidently) favors the global mimimum energy conformer (differences of 0.6%, 0.8%, and 0.5% for *A*, *B*, and *C*, respectively) over conformer 2 (differences of 2%, 2%, and 1.9% for *A*, *B*, and *C*, respectively). These data are also supported by the nuclear quadrupole coupling tensor elements, which for the lowest energy species give relative differences of 1.2%, 0.5%, and 0.9% for χ_{aa}, χ_{bb}, and χ_{cc}, respectively, whereas these percentages are 1.9%, 3.3%, and 0.5%, respectively, for the higher energy conformer.
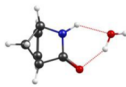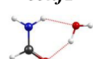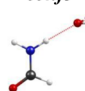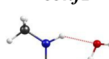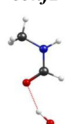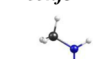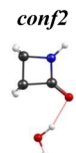
■ DISCUSSION

The spectroscopic data obtained for the Vince lactam, together with quantum chemical calculations, indicate a rather rigid bicyclo unit, with centrifugal distortion constants of relatively small magnitude and similar to those of the related exo-2-aminonorborn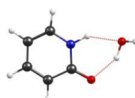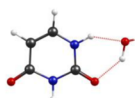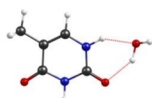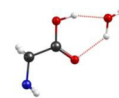ane.[9] In fact, in ABH the carbon skeleton provides a rigid framework that leaves no conformational degrees of freedom available. This is a situation similar to that

found in previously studied norbornanes[9] and tropanes,[8] in which the only conformational flexibility arises out of the carbon cyclic frame by rotation/inversion of the amino group. Consequently, the quantum mechanical predictions using MP2 and DFT methods are very consistent among themselves with average differences of 0.7% for distances and 0.3% for angles.

It is instructive to compare the experimentally observed structure of ABH in the gas phase with the crystal structure data obtained by X-ray diffraction.[25] The most relevant bond distances and angles appear in Table S9 of the Supporting Information, with atom numbering being presented in Scheme 1. When the gas-phase values are compared to solid structure data, the overall agreement is good, indicating that the structural unit keeps the same inner arrangement in the gas and solid phases. However, it should be noticed that all interatomic distances are slightly smaller in the crystal (MP2, average 1.7%) than in the equilibrium data, except for the C–O distance. The difference between the angles is smaller (0.7% on average between the crystal and MP2 data), with no clear trend. These results may indicate a certain contraction of the ABH structural unit in the solid and can be attributed to packing forces in the crystal among different ABH units, especially the hydrogen bonds between N–H and C=O groups that form ribbons.

Table 4. Computed Dissociation Energies of Several M···H$_2$O Complexes in Which the M Molecule Has an Amide Group Linked to the Water Molecule via Hydrogen Bonding[h]

	ABH-w	FOR-w[a]			mFOR-w[b]		
		conf1	*conf2*	*conf3*	*conf1*	*conf2*	*conf3*
D_0(MP2/M06-2X/B3LYP) / kJ mol^{-1}	24.6/ 33.6/ 26.7	23.8/ 33.4/ 26.3	12.3/ 21.5/ 17.8	15.1/ 17.7/ 15.0	25.0/ 36.7/ 27.9	19.5/ 27.5/ 19.7	17.2/ 23.3/ 19.2
D_e(MP2/M06-2X/B3LYP) / kJ mol^{-1}	33.6/ 43.3/ 35.8	33.7/ 45.2/ 37.1	20.1/ 31.3/ 25.6	20.8/ 24.8/ 21.3	35.6/ 45.7/ 38.1	24.8/ 32.0/ 26.7	26.9/ 35.5/ 27.8
r(CO···H) / Å	1.93	1.95	1.93		1.92	1.91	1.89
<(C=O···H) / deg	104.2	107.6	101.6		107.8	98.5	130.6
r(NH···O) / Å	2.10	2.06		2.01	2.05		
<(N-H···O) / deg	133.6	138.0		177.6	140.4		
R_{CM} / Å	3.78	2.85	3.46	4.02		3.95	3.28
k_s / kg s^{-2}	8.1	23.5	5.8	6.0		7.7	8.9
E_D / kJ mol^{-1}	9.6	16.0	5.9	8.2		10.0	8.0

	AZE-w[c]		PYR-w[d]	URA-w[e]	THY-w[f]	GLY-w[g]
	conf1	*conf2*				
D_0(MP2/M06-2X/B3LYP) / kJ mol^{-1}	24.0/ 33.2/ 25.1	18.1/ 25.6/ 19.3	33.5/ 41.6/ 36.1	30.1/ 39.5/ 31.8	31.0/ 39.5/31.3	30.5/ 38.1/ 29.4
D_e(MP2/M06-2X/B3LYP) / kJ mol^{-1}	-33.4/ -43.3/-34.5	-25.7/ -34.4/ -26.8	-41.7/ -52.0/ -46.2	39.2/ 49.6/ 41.2	39.8/ 49.4/41.0	40.3/ 47.3/39.4
r(CO···H) / Å	1.96	1.93	1.87	2.00	1.98	2.06
<(C=O···H) / deg	100.6	102.7	110.0	108.9	108.7	108.6
r(NH···O) / Å	2.20		1.93	1.93	1.94	
<(N-H···O) / deg	120.5		144.3	145.2	144.4	
r(O-H···O) / Å						1.80
<(O-H-O) / deg						156.3
R_{CM} / Å	3.30	3.49	3.70	4.25	4.40	3.62
k_s / kg s^{-2}	14.5	5.7	16.8	30.1	29.7	17.1
E_D / kJ mol^{-1}	13.2	5.8	19.2	45.4	48.1	18.7

[a]Reference 18. [b]Reference 19. [c]Reference 20. [d]Reference 23. [e]Reference 22. [f]Reference 22. [g]Reference 35. [h]FOR = formamide, mFOR = N-methylformamide, AZE = 2-azetidinone, PYR = 2-pyridone, URA = uracil, THY = thymine. The glycine−water (GLY−w) system is also included. Quantum mechanical methods include BSSE correction. Values are calculated for the most stable conformers. The bond distances and angles shown are from MP2 calculations. Pseudodiatomic model results (E_D) are also given.

A single conformer of the monohydrated ABH···H$_2$O complex has been detected and assigned to the predicted global minimum. The only evidence of large-amplitude motion comes from the free hydrogen atom, which leads to the formation of two different conformers very near in energy. Otherwise, the results suggest a reduced intermolecular dynamics and relatively strong hydrogen bonds. Similarly to other molecules with adjacent amino and carbonyl moieties, these polar groups act as molecular tweezers, accommodating the water molecule between the two donor and acceptor partners. The amphiprotic water molecule simultaneously engages as proton donor to the carbonyl group (C=O···H−O) and as acceptor through the amino group (N−H···O), forming a six-membered cooperative hydrogen bond network.[33] This particular characteristic makes the peptide bond especially prone to multiple hydration, though rotational studies are still mostly limited to mono- and dihydrated species because of

their complexity.[18−23] The largest hydrogen bond network resolved rotationally is the water hexamer.[34] According to our (MP2) calculations, the equilibrium hydrogen−oxygen distance in the O−H···O=C hydrogen bond is 1.93 Å, whereas it is 2.10 Å in N−H···O. The ABH···H$_2$O system and those water complexes studied so far can be used as probes of molecular solvation sites and can help to explain the conformational preferences of water linked to proteins. In all the studied cases the most stable conformer adopts the same conformation found in ABH···H$_2$O. N-Methylformamide···H$_2$O[19] can be taken as an exception, since it presents a *trans* configuration of the peptidic group and the *cis* species was not observed.[19]

Because of the interest in comparing the complexation energies in different water complexes, this parameter has been calculated by the ab initio and DFT methods. Table 4 presents the dissociation energies and representative geometric parameters for ABH···H$_2$O and similar structures of water complexes

linked to peptide groups (formamide, *N*-methylformamide, 2-azetidinone, 2-pyridone, uracil, and thymine).

The interatomic distances and angles shown in Table 4 indicate that hydrogen-bonding geometric parameters of ABH···H_2O lie within the range exhibited in similar water complexes, suggesting that the norbornane-based ring structure does not exert a distinctive influence in the peptide bond spatial arrangement. The spectroscopic dissociation energy of the ABH···H_2O complex (D_0) calculated with the MP2 method is 24.6 kJ/mol, which can be considered of moderate strength for hydrogen bond interaction between neutral species.[1] Table 4 shows that the presence of two cooperative hydrogen bonds in this cyclic structure tends to give higher D_0 values than noncyclic conformers, as can be seen for formamide−water, methylformamide−water, or 2-azetidinone−water. The complex dissociation energies of the cyclic conformers in all systems give very similar values, near 25 kJ/mol, suggesting that the hydrogen-bonding energy to the peptide bond is not very sensitive to the exact nature of the parent molecule. The exception is presented by six-membered cycle monomers (pyridine, uracil, and thymine), which give D_0 in the 30−34 kJ/mol range, about 10 kJ/mol higher than in the other examples in Table 4. This fact can be attributed to the extra stabilization given by the delocalized electrons in the monomer ring. The case of glycine−water,[35] which also exhibits a double hydrogen bond, but replacing a N−H···O bond by an O−H···O one, is also included in Table 4 for comparison. The dissociation energy for the most stable glycine−water conformer is 30.5 kJ/mol, i.e., about 5 kJ/mol higher than for simple systems with peptidic bonds, and is of similar magnitude compared to complexes with pyridine, uracil, and thymine. Dissociation energies computed with the B3LYP functional give values close to those of MP2, whereas the M06-2X functional gives systematically higher values (about 10 kJ/mol), suggesting that this method cannot fully reproduce the dominantly electrostatic nature of the hydrogen bond.

Table 4 also includes the complex dissociation energies estimated by assuming a pseudodiatomic model[36] for the relative displacement of the parent molecule and the H_2O subunits in the complex. For a Lennard-Jones-type intermolecular potential, the dissociation energy can be simply calculated by the formula[37] $E_D = (1/72)k_s R_{CM}^2$, where k_s is the force constant of the stretching vibrational relative motion of both subunits and R_{CM} is the distance between the centers of mass of both monomers. For asymmetric top complexes in which the stretching coordinate is nearly parallel to the *a* inertial axis, k_s can be calculated using the expression $k_s = 16\pi^4(\mu R_{CM})^2[4B^4 + 4C^4 − (B − C)^2(B + C)^2]/hD_J$, where μ is the reduced mass of the monomers, B, C, and D_J are the measured rotational constants of the complex, and h is Planck's constant. E_D values using this method have been calculated using the experimental rotational parameters and the calculated R_{CM} values from ab initio structures. Although this method does not claim to be as accurate as ab initio computations, its simplicity retains a reasonable amount of physical insight and makes it attractive for qualitative and comparison purposes. The values in Table 4 show that the essential features of dissociation energy are well reproduced by this model: cyclic-structure complexes give the highest E_D values, whereas the higher dissociation energies coming from the cyclic pyridine, uracil, and thymine monomers are also evident. Absolute magnitudes of E_D tend to be about half the quantum mechanically calculated values. However, a bigger variation of

E_D with monomer unit is predicted for the lowest lying complexes: from 9.6 kJ/mol for ABH···H_2O to 16.0 kJ/mol for formamide−water (conformer 1). This fact comes from the higher values of B and C rotational constants for the small formamide−water complex, as R_{CM} is smaller than in ABH···H_2O. Also in this method dissociation energies tend to increase as the number of atoms in the monomer unit increases, as this will tend to increase the value of R_{CM}.

With respect to the overall performance of the quantum methods, for ABH, rotational constants obtained by the MP2 method give the best agreement with experimental values, with differences below 0.1%. Both DFT methods also render a satisfactory performance, with B3LYP tending to slightly overestimate the magnitude of A, B, and C. Regarding ABH···H_2O, however, MP2 gives the biggest deviations from experimental rotational constants (about 2% in absolute value), followed by M06-2X, whereas B3LYP-calculated rotational constants are closest to the experimental values (the biggest error is 0.4%). These results suggest that the role of dispersive forces in quantum chemical calculations is quite challenging.

■ CONCLUSIONS

The Vince lactam and the lowest energy conformer of its monohydrated complex ABH···H_2O have been detected and characterized in the gas phase, and rotational constants, centrifugal distortion constants, and nuclear quadrupole coupling constants have been accurately determined. The comparison with quantum chemical calculations has unequivocally allowed determination of their structure. Results for ABH indicate a rather rigid molecular frame, as expected from its bicyclo frame. In ABH···H_2O, the amphiprotic nature of the water molecule favors the formation of a six-membered cooperative hydrogen bond network. Hydrogen-bonding geometric parameters of ABH···H_2O lie within the range exhibited in similar water complexes, leading to the conclusion that the norbornane-based ring structure does not exert a distinctive influence in the peptide bond spatial arrangement. The calculated spectroscopic dissociation energy of the ABH···H_2O complex (24.6 kJ/mol) indicates a moderately strong hydrogen bond interaction and is comparable to the dissociation energies of similar cyclic complexes detected so far. These results suggest that the hydrogen-bonding energy to the peptide bond of the most stable conformers is rather insensitive to the exact nature of the parent molecule, with the exception of six-membered ring monomers, in which extra stabilization seems to be given by electrons from the ring. Quantum calculations, performed at the MP2 and DFT (B3LYP and M06-2X) levels of theory, reproduce the experimental spectroscopic parameters satisfactorily overall, although noticeable differences between experimental and calculated rotational constants in ABH···H_2O suggest that quantum chemical calculations involving hydrogen-bonded systems are still quite challenging. This work shows that the ABH···H_2O system, together with other water complexes studied so far, can be used as a probe of molecular solvation sites and can help to explain the conformational preferences of water linked to proteins.

■ ASSOCIATED CONTENT

Ⓢ Supporting Information

Tables S1−S9 and Figure S1 as mentioned in the text. This material is available free of charge via the Internet at http://pubs.acs.org.

■ AUTHOR INFORMATION

Corresponding Author

*Phone: +34 94 601 2532 (F.J.B.); +34 94 601 5387 (E.J.C.). Fax: +34 94 601 3500 (F.J.B.). E-mail: franciscojose. basterretxea@ehu.es (F.J.B.); emiliojose.cocinero@ehu.es (E.J.C.). URL: http://www.grupodeespectroscopia.es/MW (F.J.B., E.J.C.).

Notes

The authors declare no competing financial interest.

■ ACKNOWLEDGMENTS

■ REFERENCES

(1) Schermann, J. P. *Spectroscopy and Modeling of Biomolecular Building Blocks*; Elsevier: Amsterdam, 2008.

(2) Gerothanassis, I. P. *Prog. NMR Spectrosc.* **1994**, *26*, 171−237.

(3) Marechal, Y. *The Hydrogen Bond and the Water Molecule: The Physics and Chemistry of Water, Aqueous and Bio-Media*; Elsevier: Amsterdam, 2007.

(4) Cocinero, E. J.; Gamblin, D. P.; Davis, B. G.; Simons, J. P. *J. Am. Chem. Soc.* **2009**, *131*, 11117−11123.

(5) Stanca-Kaposta, E. C.; Gamblin, D. P.; Cocinero, E. J.; Frey, J.; Kroemer, R. T.; Fairbanks, A. J.; Davis, B. G.; Simons, J. P. *J. Am. Chem. Soc.* **2008**, *130*, 10691−10696.

(6) Caminati, W.; Grabow, J.-U. In *Frontiers of Molecular Spectroscopy*; Laane, J., Ed.; Elsevier: Amsterdam, 2008; Chapters 14 and 15.

(7) Banser, D.; Schnell, M.; Grabow, J. U.; Cocinero, E. J.; Lesarri, A.; Alonso, J. L. *Angew. Chem., Int. Ed.* **2005**, *44*, 6311−6315.

(8) Cocinero, E. J.; Lesarri, A.; Écija, P.; Grabow, J.-U.; Fernández, J. A.; Castaño, F. *Phys. Chem. Chem. Phys.* **2010**, *12*, 6076−6083.

(9) Écija, P.; Cocinero, E. J.; Lesarri, A.; Millán, J.; Basterretxea, F. J.; Fernández, J. A.; Castaño, F. *J. Chem. Phys.* **2011**, *134*, 164311/1−164311/8.

(10) Cocinero, E. J.; Lesarri, A.; Écija, P.; Grabow, J.-U.; Fernández, J. A.; Castaño, F. *Phys. Chem. Chem. Phys.* **2010**, *12*, 12486−12493.

(11) Cocinero, E. J.; Lesarri, A.; Écija, P.; Basterretxea, F.; Fernández, J. A.; Castaño, F. *J. Mol. Spectrosc.* **2011**, *267*, 112−117.

(12) Cocinero, E. J.; Basterretxea, F. J.; Écija, P.; Lesarri, A.; Fernández, J. A.; Castaño, F. *Phys. Chem. Chem. Phys.* **2011**, *13*, 13310−13318.

(13) Cocinero, E. J.; Lesarri, A.; Écija, P.; Basterretxea, F. J.; Grabow, J.-U.; Fernández, J. A.; Castaño, F. *Angew. Chem., Int. Ed.* **2012**, *51*, 3119−3124.

(14) Daluge, S.; Vince, R. *J. Org. Chem.* **1978**, *43*, 2311−2320.

(15) Vince, R.; Hua, M. *J. Med. Chem.* **1990**, *33*, 17−21.

(16) Rommel, M.; Ernst, A.; Koert, U. *Eur. J. Org. Chem.* **2007**, *26*, 4408−4430.

(17) Novak, I.; Huang, W. *J. Phys. Org. Chem.* **1999**, *12*, 388−391.

(18) Blanco, S.; López, J. C.; Lesarri, A.; Alonso, J. L. *J. Am. Chem. Soc.* **2006**, *128*, 12111−12121.

(19) Caminati, W.; López, J. C.; Blanco, S.; Mata, S.; Alonso, J. L. *Phys. Chem. Chem. Phys.* **2010**, *12*, 10230−10234.

(20) (a) López, J. C.; Blanco, S.; Sánchez, R.; Lesarri, A.; Alonso, J. L. 60th International Symposium on Molecular Spectroscopy, Columbus, OH, 2007; Communication FC07. (b) Sánchez, R. Ph.D. Thesis, Universidad de Valladolid, 2005.

(21) Vaquero, V.; Sanz, M. E.; López, J. C.; Alonso, J. L. *J. Phys. Chem. A* **2007**, *111*, 3443−3445.

(22) López, J. C.; Alonso, J. L.; Peña, I.; Vaquero, V. *Phys. Chem. Chem. Phys.* **2010**, *12*, 14128−14134.

(23) Maris, A.; Ottaviani, P.; Caminati, W. *Chem. Phys. Lett.* **2002**, *360*, 155−160.

(24) Novak, I.; Kovač, B. *Spectrochim. Acta, A* **2005**, *61*, 1007−1009.

(25) Suchod, B.; Lajzerowicz, J.; Collet, A. *Acta Crystallogr.* **1997**, *C53*, 1911−1912.

(26) Balle, T. J.; Flygare, W. H. *Rev. Sci. Instrum.* **1981**, *52*, 33−45.

(27) Jensen, F. *Introduction to Computational Chemistry*; John Wiley & Sons: Chichester, U.K., 2007.

(28) Zhao, Y.; Truhlar, D. G. *Theor. Chem. Acc.* **2008**, *120*, 215−241.

(29) Zhao, Y.; Truhlar, D. G. *Acc. Chem. Res.* **2008**, *41*, 157−167.

(30) Frisch, M. J.; Trucks, G. W.; Schlegel, H. B.; Scuseria, G. E.; Robb, M. A.; Cheeseman, J. R.; Scalmani, G.; Barone, V.; Mennucci, B.; Petersson, G. A.; et al. *Gaussian 09*, revision A02; Gaussian Inc.: Wallingford, CT, 2009.

(31) Gordy, W.; Cook, R. L. *Microwave Molecular Spectra*; Wiley: New York, 1984.

(32) Watson, J. K. G. In *Vibrational Spectra and Structure*; Durig, J. R., Ed.; Elsevier: Amsterdam, 1977; Vol. 6, pp 1−89.

(33) Jeffrey, G. A. *An Introduction to Hydrogen Bonding*; Oxford University Press: Oxford, U.K., 1997.

(34) Pérez, C.; Muckle, M. T.; Zaliski, D. P.; Seifert, N. A.; Temelso, B.; Shields, G. C.; Kisiel, Z.; Pate, B. H. *Science* **2012**, *336*, 897−901.

(35) Alonso, J. L.; Cocinero, E. J.; Lesarri, A.; Sanz, M. E.; López, J. C. *Angew. Chem., Int. Ed.* **2006**, *45*, 3471−3474.

(36) Millen, D. *Can. J. Chem.* **1985**, *63*, 1477−9.

(37) Novick, S. E.; Harris, S. J.; Janda, K. C.; Klemperer, W. *Can. J. Phys.* **1975**, *53*, 2007−2015.